Protein Transport upon Advection at the Air/Water Interface: When Charge Matters

Coralie Pasquier, Stéphane Pezennec, Antoine Bouchoux, Bernard Cabane, Valérie Lechevalier-Datin, Cécile Le Floch-Fouéré, G. Paboeuf, Maryvonne Pasco, Benjamin Dollet, Lay-Theng Lee, et al.

Protein transport upon advection at the air/water interface: when charge matters

*Coralie. Pasquier[1,2,§], Stéphane. Pezennec[1], Antoine. Bouchoux[3], Bernard. Cabane[4], Valérie. Lechevalier[1], Cécile. Le Floch-Fouéré[1], Gilles. Paboeuf[2,7], Maryvonne. Pasco[1], Benjamin. Dollet[5], Lay-Theng. Lee[6], Sylvie. Beaufils[2,7]**

1 INRAE, Institut Agro, STLO, F-35042, Rennes, France

2 IPR Institute of Physics, UMR UR1 CNRS 6251, Rennes 1 University, France

3 TBI, Université de Toulouse, CNRS, INRAE, INSA, Toulouse, France

4 LCMD, CBI, ESPCI - Paris Tech, 75231 Paris, France

5 Univ. Grenoble Alpes, CNRS, LIPhy, 38000 Grenoble, France

6 Laboratoire Léon Brillouin CEA - Saclay 91191, Université Paris-Saclay, Gif-sur-Yvette Cedex, France

7 Univ Rennes 1, CNRS, ScanMAT – UMS 2001 F-35042 Rennes, France

* *corresponding author*

§ present address: Institut de Chimie Séparative de Marcoule (ICSM), UMR 5257 (CEA, CNRS, UM, ENSCM), 30207 Bagnols-sur-Cèze, France

Corresponding author sylvie.beaufils@univ-rennes1.fr

ABSTRACT

The formation of dense protein interfacial layers at a free air-water interface is known to result from both diffusion and advection. Furthermore, proteins interactions in concentrated phases are strongly dependent on their overall positive or negative net charge, which is controlled by the solution pH. As a consequence, an interesting question is whether or not the presence of an advection flow of water towards the interface during protein adsorption produce different kinetics and interfacial structure of the adsorbed layer, depending on the net charge of the involved proteins and, possibly, on the sign of this charge. Here we test a combination of the following parameters using ovalbumin and lysozyme as model proteins: positive or negative net charge, presence or absence of advection flow. The formation and the organization of the interfacial layers are studied by neutron reflectivity and null-ellipsometry measurements. We show that the *combined* effect of a positive charge of lysozyme and ovalbumin and the presence of an advection flow is necessary to induce interfacial multilayers formation. Conversely, negatively charged ovalbumin forms monolayers, whether an advection flow is present or not. We show that an advection/diffusion model cannot describe correctly the adsorption kinetics of multilayers, even in the hypothesis of a concentration-dependent diffusion coefficient like in colloidal filtration for instance. Still, it is clear that advection is a necessary condition for making multilayers through a mechanism that remains to be determined, which paves the way for future research.

Keywords: *protein, ovalbumin, lysozyme, monolayers, multilayers, neutron reflectivity, null-ellipsometry, advection-diffusion, adsorption, air-water interface.*

Introduction

Proteins in solution form films by accumulation towards hydrophobic interfaces[1–4].These interfaces in turn control the behavior of a wide variety of synthetic or natural systems such as technological

Corresponding author sylvie.beaufils@univ-rennes1.fr

foams and emulsions[5–9]. Liquid foams stabilized by proteins are for instance hugely present in the food industry food industry[10] and therefore extensively .extensively studied by researchers[11]. The field of biomaterials is also concerned by protein adsorption on various surfaces[12] and hydrophobic interfaces are also found *in vivo*, where proteins for instance adsorb at the liquid-air interface which acts as a barrier for a wide range of organisms[13]. In addition, membrane-based techniques are frequently used for the separation and purification of proteins[14], as milk filtration, for instance[15–17]. The formation of a monolayer of protein adsorbed onto the membranes generally impairs the performance of the filtration and is this time a negative phenomenon that needs to be avoided[18]. These numerous fields of application explain why adsorption mechanisms related to protein films formation and the structure of such films have been and are still widely studied (see Yano 2012[19] for a review). Among the parameters which control the formation of the protein interfacial film, we can of course identify diffusion and convection, the latter being due to inhomogeneities in physical parameters (such as temperature) in the bulk and to internal fluid movement. Diffusion and convection act in conjunction during the first steps of the film formation, and many authors have mentioned the importance of early convection mechanisms in the formation of the interfacial layer[1,20–22]. However, it is well-known that evaporation induces advection (i.e. convection toward the interface) in bulk liquids and can be at the origin of spectacular effects such as the tears of wine for instance[23], or the coffee stain effect[24], where the evaporation-induced advection velocity has been measured. directly[25].

Accordingly, an interesting question is wether or not evaporation - and the associated advection flux - has an impact on the adsorption of proteins at interfaces. It is all the more interesting that it corresponds to numerous real situations when a permanent evaporation/advection flow is maintained across the interface (e.g. in case of an open air surface). In these cases, we still do not have a clear picture of how the protein interfacial film continues to evolve because of advection. Also in such a situation, one important parameter that needs to be taken into account is the *charge* of the involved proteins; a characteristic that is known to directly affect film formation[26–30] - and therefore quite

Corresponding author sylvie.beaufils@univ-rennes1.fr

potentially the evolution of the film upon advection. By *charge*, we mean not only the *net electrical charge* of the protein, as it is often only considered in the literature, but also the *sign* of the charge (+/). An increasing number of reports now indicate that protein interactions - hence interfacial film formation - also depend on forces that are controlled by the *sign* of this charge rather than its absolute value[31–34].

To summarize, our objective here is to investigate the combined effects of *protein charge* (sign and net charge) and *advection* on the formation and evolution of protein films at an hydrophobic interface (here the air-water interface). Some of our specific questions are: what is the impact of a permanent advection flow on the film formation? Does the sign of the proteins have an importance in this context?

As models, two well-known proteins are considered separately: ovalbumin and lysozyme. Their adsorption at the air-buffer interface is studied by neutron reflectivity and null-ellipsometry, with and without permanent advection flow and for positive and negative net electric charge in case of ovalbumin.

EXPERIMENTAL

Sample preparation

Lysozyme hydrochloride powder (lysozyme purity higher than 98%, as determined by reversed-phase high-performance liquid chromatography (HPLC)) was a gift from LIOT (Annezin, France).

Ovalbumin was purified from hen egg white according to the protocol described by Croguennec[35]. Egg white was separated from whole eggs and diluted three times with 15 MΩ cm purified water prepared by reverse osmosis, before adjusting the solution pH to 6.0 with HCl and keeping it overnight at 5°C, under agitation. The next day, the pH was adjusted again to 6.0 and the solution

Corresponding author sylvie.beaufils@univ-rennes1.fr

was centrifuged at 2000×*g*, 5°C for 4 minutes. The supernatant pH was adjusted to 8.2 with NaOH, before centrifugation at 25900×*g*, 4°C, for 20 minutes. The supernatant, a mucin-free egg white solution, was then collected and weighted.

Ovalbumin was then extracted from the solution via anion-exchange chromatography, performed on a LRC column (Pall Life Sciences, Port Washington, USA) packed with Q-Sepharose Fast Flow media (Pharmacia Biotech AB, Uppsala, Sweden). Three solutions were successively run through the column: a 0.035 M NaCl solution (extraction of unwanted proteins), then a 0.14 M NaCl solution (extraction of ovalbumin), then a 1 M NaCl solution (cleaning of the column). Protein concentration was monitored by measuring optical absorption at 280 nm with a UV 325 Dual Wavelength UV-Vis Detector (Agilent Technologies, Santa Clara, USA), using an adsorption coefficient of $\varepsilon = 2.93 \times 10^4\ \mathrm{M^{-1}\ cm^{-1}}$.

Ovalbumin solutions were then dialyzed for 3 days against several successive baths of 15 MΩ cm purified water, then centrifuged and freeze-dried for storage.

Protein charges were computed with the PDB2PQR [36] and PROPKA[37] software from the lysozyme and ovalbumin structures (PDB ID 1HEL and 1OVA, respectively). Table T-1 summarizes protein charge values, in supplementary materials.

Bulk solutions and buffer

Solutions of ovalbumin and lysozyme were prepared at a 1 $g.L^{-1}$ concentration in buffered deuterium oxide D_2O. The deuterium analog of pH in D_2O solutions, pD, was measured by adding 0.4 to the pH-meter reading, after standardization of the electrode in H_2O buffers[38]. Ionic strength I=20 mM, pD 7.0 buffer was prepared using 11.3 mM bis-tris propane (1,3-bis(tris(hydroxymethyl)methylamino)propane, Sigma-Aldrich, St-Louis, USA) adjusted to pD 7.0

Corresponding author sylvie.beaufils@univ-rennes1.fr

with HCl. *I*=20 mM, pD 3.6 buffer was prepared using 56.4 mM lactic acid-sodium lactate. *I*=170 mM buffers were prepared by adding 150 mM NaCl to the *I*=20 mM buffers.

Neutron reflectivity

Specular neutron reflectivity experiments were carried out on the time-of-flight neutron reflectometer G3bis at the ORPHEE reactor (Laboratoire Léon Brillouin, CEA-Saclay) using a polychromatic beam with wavelength $\lambda \approx 2.5$ to 25 Å. The incident beam was bent with a supermirror onto the liquid surface at a grazing incident angle $\theta = 1.54°$ with angular resolution $\delta\theta/\theta \approx 0.05$ as calibrated with pure D_2O, giving a corresponding wave vector range $Q = 4\pi sin\theta/\lambda$ of about 0.014 to 0.14 Å^{-1}. Under this configuration, there is adequate total reflection plateau from the deuterated solvent subphase for $Q < Q_c \approx 0.018$ Å^{-1} where Q_c is the critical total reflection edge. The sample container was a Teflon trough (35 mm×95 mm) that was enclosed in an air-tight aluminum cell with quartz windows to allow the neutron beam to pass through with minimal absorption. The cell was equipped with a temperature control system to monitor the experimental temperature to T = 20.0 °C ± 0.2 °C and the entire setup was positioned on an anti-vibration support. Most measurements were carried out under this hermetically-enclosed condition hence no advective flow due to evaporation took place during the measurements. Some experiments were also performed without the cover of the trough (called "free surface configuration") to allow evaporation and advective flow during the measurements. Reflectivity spectra were acquired at one or two-hour intervals.

The basic principles of neutron reflectivity have been discussed in detail in several past literature[39–41]Experimentally, reflectivity is measured as a function of of Q and $R(Q) = I\,(Q)/I_0\,(Q)$, where $I(Q)$ and $I_0(Q)$ are intensities of the reflected and the incident beam, respectively. The reflectivity profile depends on the neutron refractive index profile normal to the surface $n(z)$ which is defined (neglecting absorption) as: $n(z) = 1 - (Nb\,(z)/2\,\pi)\lambda^2$ where z is the distance from the interface,

Corresponding author sylvie.beaufils@univ-rennes1.fr

$Nb(z)$ is the scattering length density given by $Nb = \sum_j b_j n_j$ where b_j is the neutron scattering length and n_j the number density of the atomic species j. The difference in scattering length density of the proteins and the deuterated buffer is negative. For lysozyme, $\Delta Nb = Nb_p - Nb_s$ = -2.67 x 10^{-6} $Å^{-2}$where Nb_p = 3.65 × 10^{-6} $Å^{-2}$ is the theoretically calculated scattering length density of the protein using densityρ = 1.43 g·cm^{-3} [7] and taking into account H-D exchange of labile hydrogen; Nb_s = 6.32 × 10^{-6} $Å^{-2}$ is the experimentally determined scattering length density of the deuterated buffer solution. The corresponding values for ovalbumin are: ΔNb= -3.26 × 10^{-6} $Å^{-2}$ where Nb_p = 3.07×10^{-6} $Å^{-2}$ and ρ = 1.36 g·cm^{-3}. In the presence of an adsorbed protein layer, the reflectivity is thus decreased with respect to that of the pure solvent and therefore the normalized reflectivity gives $R/R_F < 1$. R_F is the reflectivity of the deuterated buffer solution taking into account angular resolution. In this work, all reflectivity spectra are expressed in the normalized form, R/R_F. In this representation, all deviations of R/R_F from unity are attributed only to the adsorbed layer, and the higher the adsorption, the larger is the deviation from unity.

Data analysis: The reflectivity curves are modeled using an *n-slice* step function of uniform scattering length density given by:

$$Nb(z) = \sum_{0}^{N} \left(\frac{Nb_i - Nb_{i+1}}{2}\right)\left(1 - erf\,\frac{(z - z_i)}{\sigma_i}\right)$$

Nb_i is the scattering length density and $z_i - z_{i+1}$ the thickness (d_i) of slice i, and σ_i is the interfacial roughness between slice i and i+1 described by an error function. n = 0 and $n = N$ represent the two semi-infinite media air and bulk buffer, respectively. The adjustable parameters are Nb_i, d_i and σ_i. In a first fitting, σ_i is found to fall between 0.3 to 2.3 Å with the majority falling around 0.7 – 1.5 Å, except for the innermost roughness (between the last layer and the subphase) that gives larger variations depending on the protein volume fraction and thickness of the layer. In order to reduce the number of fitting parameters, σ_i is fixed at 1 Å except for the innermost roughness which is allowed

Corresponding author sylvie.beaufils@univ-rennes1.fr

to float; the fitted values of this last roughness range from about 2 to 8 Å (increasing with the thickness of the slice). The best-fit parameters are determined by iteration and minimization of the χ^2 parameter between the experimental and theoretical curves. From the fitted scattering length density profile $Nb(z)$, the protein density profile $\phi(z)$ can be estimated using the relations: $Nb = \phi_p Nb_p + \phi_s Nb_s$ and $\phi_p + \phi_s = 1$. Nb is the fitted scattering length density, Nb_p and Nb_s are as defined above, and ϕ_p and ϕ_s are the volume fractions of protein and solvent respectively. Note that the expression of the *n-slice* profile refers to an adsorbed interfacial layer that can be described by *n* regions of uniform scattering length density each (in the *z*-direction); it does not necessarily correspond to *n* molecular layers.

Ellipsometric measurements at the air-water interface

Adsorption layers were prepared on a circular trough, the surface of which (S=25 cm^2) is directly in contact with air. Hence, an advective flow develops during adsorption kinetics. The speed of the evaporation front (ie flux density) was estimated through the recording of the evaporated mass of water with time; its value was found to be constant, equal to 21 $nm.s^{-1}$. The ellipsometric measurements were carried out with a home-made ellipsometer, in the so-called "null-ellipsometer configuration" operated with He–Ne laser (λ=632.8 nm, Melles Griot, Carlsbad, CA) that was polarized with a Glan-Thompson polarizer. The incidence angle of the light on the surface was fixed, equal to 1° away from the Brewster angle. The laser beam probed a surface of 1 mm^2 and a depth of the order of 1 μm.

After reflection on the water surface, the laser light passed through a λ/4 retardation plate, a Glan-Thompson analyzer, and a photomultiplier. Through a computer-controlled feedback loop, the analyzer and the polarizer automatically rotated towards the extinction position, giving the two ellipsometric angles Δ and ψ.

Corresponding author sylvie.beaufils@univ-rennes1.fr

In case of ellipsometric measurements on the air-water interface, adsorbed layers are transparent (<10 nm) with low refractive index contrast and the angle of incidence of the laser beam is fixed. In that case, the ellipsometric angle Δ changes when the layer is formed while relative changes of the other angle ψ remain of low magnitude. We used the ellipsometric angle Δ to semi-quantitatively measure the protein amount adsorbed at the air-water interface. Depending on the protein and the physical-conditions of the buffer, a 10° ellipsometric angle Δ corresponds to protein concentrations between 0.5-2 $mg.m^{-2}$ (ref [42] and Figs.2 and 4,5).

For each kinetic measurement, initial values of the ellipsometric angle (Δ_0) and surface tension of pure buffer solutions were recorded on the subphase for at least half an hour. These values have been subtracted from all data presented below. Then, the buffer solution was removed and the protein solution was poured in the trough. Values of Δ and surface pressure (Π) were recorded every 4 s with a precision of ±0.5° and ±0.5 mN/m, respectively.

Ellipsometry was performed at least in duplicate for each analysed condition in independent experiments. The overall uncertainty of ellipsometric measurements, as estimated from replicate experiments (at least three replicates), can essentially be attributed to the variability of protein adsorption and was thus estimated from replicates to be +/- 1° for Δ in case of monolayers and much more (20°-30°) when multilayers are formed, this point being discussed below.

Additionnaly, a set of ellipsometric measurements without advective flow was performed by pouring the protein solution in a closed glass container.

RESULTS AND DISCUSSION

Positively charged lysozyme, adsorption at low ionic strength

Figure 1a shows R/R_F, measured by neutron reflectivity, for adsorption of lysozyme at pD 7, (ie net charge +8), I=20 mM, as a function of time, in the airtight trough. The solid lines are best-fit

Corresponding author sylvie.beaufils@univ-rennes1.fr

theoretical curves calculated using the corresponding density profiles shown in Figure 1b with a model consisting of "boxes" or "slices" the stack of which constitutes the physical layer. The adsorption process continues to evolve over several hours. The adsorbed layer, at the initial stage of formation (after 2 h), is best described by a two-slice model, a first slice of intermediate volume fraction ϕ_1~0.3 and thickness d_1~24 Å, and a second dilute slice of volume fraction ϕ_2~0.1 and thickness d_2~22 Å. With increase in adsorption time, ϕ_1 increases but saturates at a value ϕ_1~0.4 after 4 h; the corresponding thickness also remains almost constant at d_1~24–25 Å. The second slice however continues to grow and to reorganize with time; after 10 h a two-slice model becomes inadequate and a three-slice model is necessary to fit the reflectivity data. Thus, the adsorption process can be modelled by the formation of a first slice that is saturated within 4 h and subsequent additional slices that continue to grow over a longer period of time. All the fitted values are contained in table I.

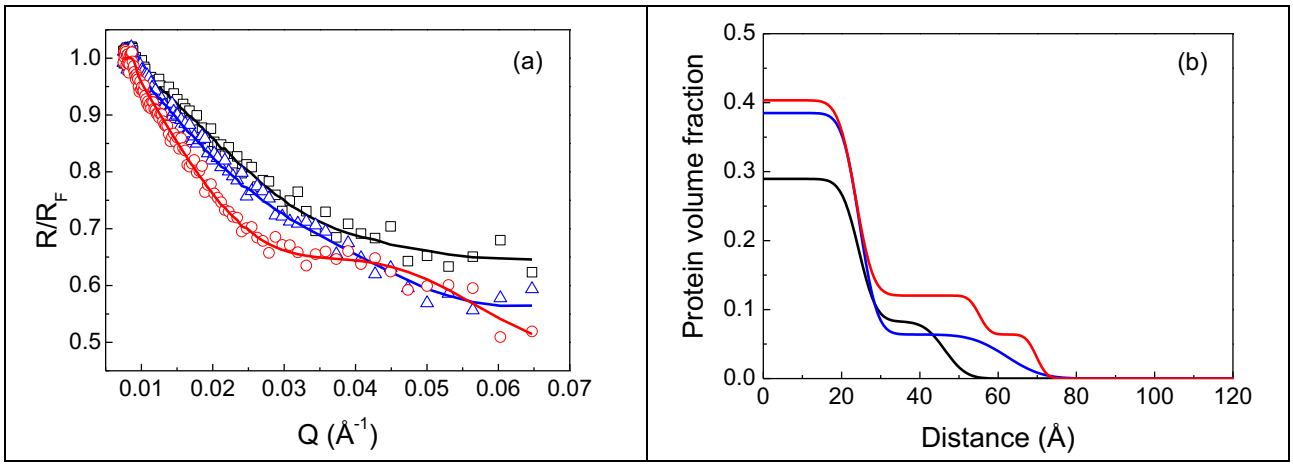

Figure 1. Kinetics of adsorption of lysozyme from D_2O at pD 7 (net charge +8) and *I*=20 mM measured by neutron reflectivity in airtight trough (without advective flow). (a) Normalized reflectivity after 2h (black squares), 4h (blue triangles), 10h (red circles); the solid lines are best-fit curves with the corresponding concentration profiles shown in (b) (same color code).

Similar measurements were performed without the cover of the trough, in the "free surface configuration" to allow for evaporative advection. (see SI-1 for R/R_F and concentration profiles). In this case, the adsorption process continues to evolve over several hours. The R/R_F curves at high- Q

Corresponding author sylvie.beaufils@univ-rennes1.fr

show an upward turn that indicates an impending weak oscillation that arises from the formation of a thick layer, the interference fringes of which are detected within the Q-range of the measurement. The weak and unusual shape of the oscillation are due to the dilute nature of the layer and a non-homogeneous internal structure, as evidenced by the three-step concentration profile (see SI). The adsorbed layer, at the initial stage of formation (after 1 h), is best described by a two-slice model, a first slice of intermediate volume fraction ϕ_1~0.35 and thickness d_1~20 Å, and a second dilute slice of volume fraction ϕ_2~0.05 and thickness d_2~50 Å. With increase in adsorption time, ϕ_1 increases up to a value ϕ_1~0.4 after 7 h (the corresponding thickness remains almost constant around d_1~20 Å) while two other slices are necessary to describe the whole profile, the volume fraction of which increases without evidence of saturation at 7 h. Note that for this open configuration, there is significant absorption of water vapor by the D_2O subphase, resulting in a decrease in the solvent scattering length density from 6.32 to 4.32 x 10^{-6} $Å^{-2}$ after 7h. This effect reduces progressively the contrast between the protein and the solvent, and consequently increases the uncertainty in the measured values (as can be seen by the large error bars). For each reflectivity curve with time, it is necessary to re-evaluate Nb_s from the critical total reflection edge, $Q_c = 4\sqrt{\pi Nb_s}$. In the data fitting, the modified values of Nb_s and Nb_p with time are taken into account and the corresponding R_F calculated accordingly. Due to this constantly changing protein-solvent contrast between spectra, the relative changes in adsorption cannot be perceived qualitatively from the R/R_F curves, and these constant changes might also contribute to the unusual appearances of the curves.

In each model slice, the surface concentration excess Γ (in mass per unit area) can be calculated from: $\Gamma = \phi_p \times d \times \rho$ where ϕ_p is the protein volume fraction in the slice, d the thickness of the slice and ρ the protein volumetric mass. The contributions of all slices are summed up to give the overall surface concentration excess in the adsorbed layer.

Corresponding author sylvie.beaufils@univ-rennes1.fr

The adsorption densities of lysozyme at *I*=20 mM are shown on Figure 2a for the airtight trough and the free surface configuration. In the latter case, it can be noticed that the excess surface density increases with time, without evidence of saturation.

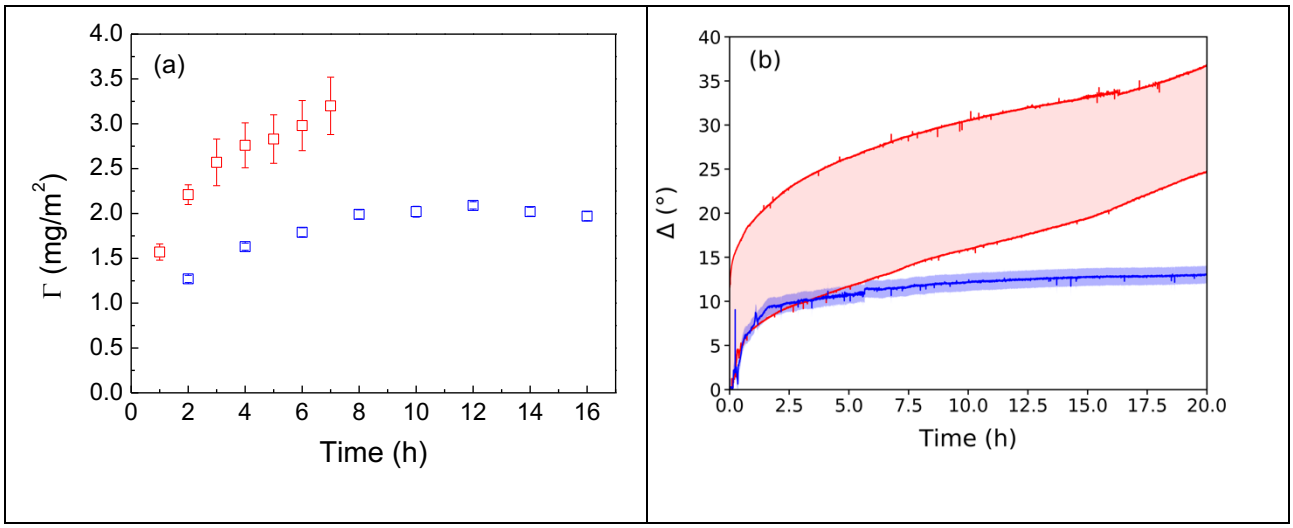

Figure 2. (a) Adsorption density versus time of lysozyme at pD 7 (net charge +8) and *I* = 20 mM without advective flow (blue squares) and with advective flow (red squares) measured by neutron reflectivity. (b) Ellipsometry measurements: ellipsometric angle *Δ* without advective flow (red lines) and with advective flow (blue line); the colored filled area shows the spread from three replicates.

Fig. 2.b shows plot of the ellipsometric angle *Δ* as a function of the adsorption time, for lysozyme at pH 7.0, *I*=20 mM, in free surface trough (with advective flow) and in the airtight trough (without advective flow). The same trends as for reflectivity measurements are noticed: without an advective flow, the kinetics show a saturation, around *Δ*=10°, which corresponds to a surface concentration of 2 mg.m^{-2}, consistent with a saturated globular protein monolayer. The reproducibility is good, as indicated by the error bar corresponding to the two replicates. In the presence of a constant advective flow, the ellipsometric angle *Δ* increases considerably faster at initial times and then monotonically increases with time without reaching saturation. A huge variability is then observed, as shown by the color filled area containing the third replicates. As this variability is only observed in these conditions, it proves that it comes from the sample and not from the apparatus. We hypothesis that the interface

Corresponding author sylvie.beaufils@univ-rennes1.fr

is highly heterogeneous in these conditions and, as the laser probes a surface of 1mm^2, the Delta value depends strongly on the thickness of the point of impact of the laser.

Positively charged Lysozyme, adsorption at high ionic strength

Figure. 3 shows the effect of NaCl on the adsorption of lysozyme at pD 7, (net charge +8), *I*=170 mM, measured by neutron reflectivity in the airtight trough (*i.e.* without advective flow). (R/R_F curves are given in SI-2). Under these conditions, adsorption is increased, as expected from the charge screening effect. Note that this screening effect, under quasi-equilibrium condition, is manifested in the densification of the dilute distal slices d_2 and d_3 only; the first slice d_1, already saturated at ϕ_1~0.4, remains insensitive to the increase in ionic strength. At the initial stage of adsorption however, (2 h, inset in Figure. 3a), increased ionic strength also increases the rate of organization in d_1 to reach faster saturation.

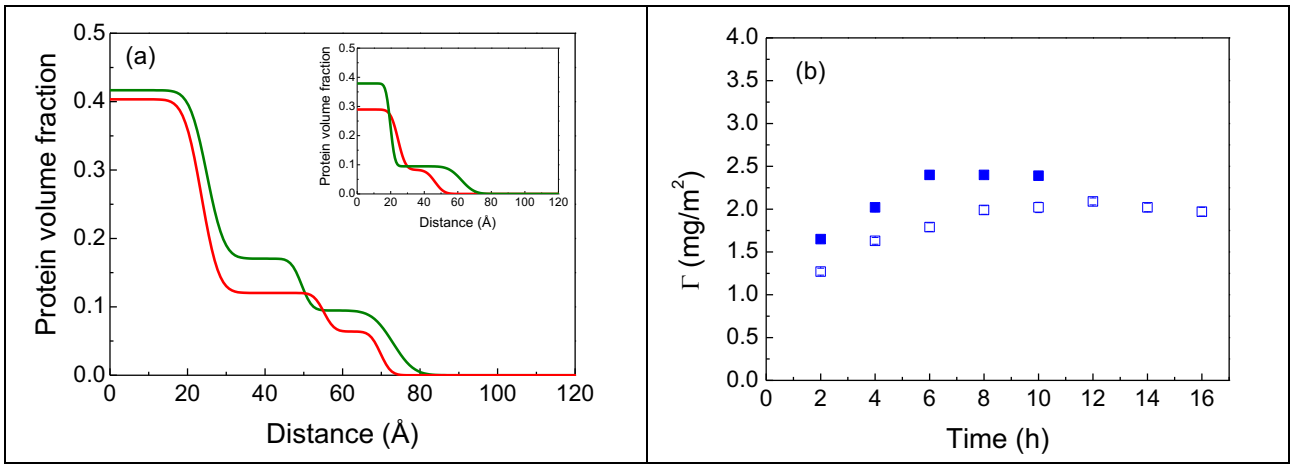

Figure 3. Effect of NaCl on adsorption of lysozyme measured by neutron reflectivity in airtight trough (without advective flow) at pD 7 (net charge +8). (a) Concentration profiles after 10h at *I* = 20 mM (red line) and *I* = 170 mM (green line); the inset shows the corresponding effect of NaCl on adsorption at shorter time (after 2 h), same color code. (b) Adsorption density versus time at *I* = 20 mM (open rectangles) and *I* = 170 mM (closed rectangles).

Corresponding author sylvie.beaufils@univ-rennes1.fr

The adsorption densities show clearly that in the presence of NaCl, the adsorption is (i) faster, since it saturates after 6 h against 10h at low ionic strength, and (ii) higher, with a surface concentration excess of 2.3 mg·m^{-2} for *I*=170 mM compared to 2.0 mg·m^{-2} for *I*=20 mM.

Positively charged ovalbumin, adsorption at low ionic strength

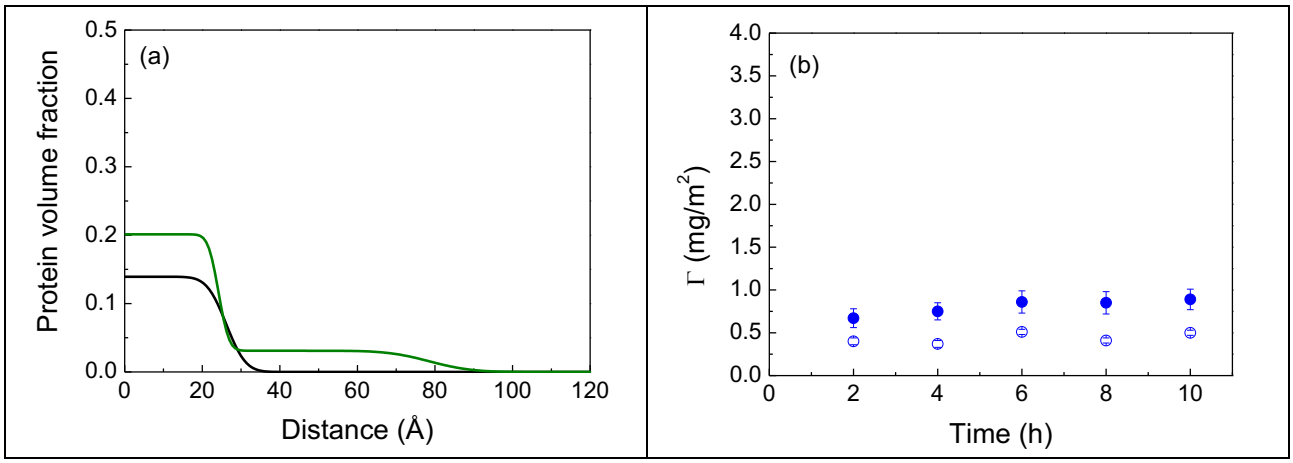

Figure 4. Effect of NaCl on adsorption of ovalbumin measured by neutron reflectivity (without advective flow) at pD 3.6 (net charge +28). (a) Concentration profiles after 10h at *I* = 20 mM (black line) and 170 mM (green line). (b) Adsorption density versus time at *I* = 20 mM (open circles) and *I* = 170 mM (closed circles).

Figure 4 shows adsorption of ovalbumin at pD 3.6, (net charge +28), I=20 mM, measured by neutron reflectivity as a function of time in the airtight trough. On Figure 4a and 4b, the Y-scales have been maintained to the same value as the previous graphs to facilitate comparisons. The adsorption density under these conditions is very low and a one-slice model adequately fits the reflectivity curve (R/RF shown in SI-3).

Figure 5 shows the plot of the ellipsometric angle Δ as a function of adsorption time, for ovalbumin at pH 3.6, *I*=20 mM, in the free surface trough (with advective flow) and in the airtight trough (without advective flow). Without advective flux, saturation is reached within 2-3 hours, which is a bit slower but still in the same range than lysozyme in comparable conditions (Fig. 2b) with the same reproducibility shown by the colored filled area.

Corresponding author sylvie.beaufils@univ-rennes1.fr

In the presence of an advective flow (we only have ellipsometry results here as neutron experiments were not performed in open-air conditions for ovalbumin at pH 3.6), we also find a behavior that is comparable with lysozyme (Fig.2b), with a strong variability, suggesting an heterogeneous layer (the colored filled area contains the three replicates), a very fast adsorption at initial times, and then a monotonic increase in adsorption with time over hours.

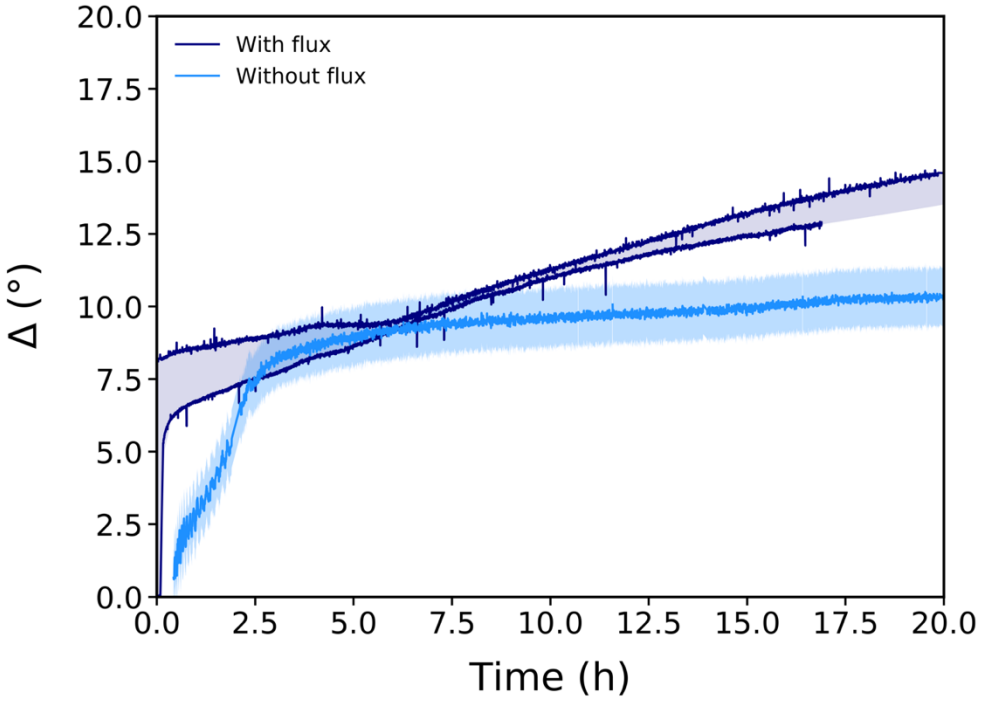

Figure 5 Ellipso nin at pH 3.6, I = 20 mM without advective flow (light blue line), the repetability shown by the co advective flow (dark blue line) where the colore filled area shows the spread of three replicates.

Positively charged Ovalbumin, adsorption at high ionic strength

At pD 3.6 when the ionic strength is increased to 170 mM using NaCl, adsorption increases, as expected due to Debye screening, and a two-slice model is required to fit the data (Fig.4). Note that at pD 3.6 and I=170 mM, although d_1 is about the same value as for lysozyme at pD 7 and I=20 mM, ϕ_1 does not reach the same extent of saturation.

Corresponding author sylvie.beaufils@univ-rennes1.fr

Negatively charged ovalbumin, adsorption at low ionic strength

The adsorption kinetics and evolution of the structure within the adsorbed layer for ovalbumin at pD 7 (net charge -10) and *I*=20 mM in airtight trough (without advective flow) are shown in Figure 6. The adsorption characteristics are similar to those observed for lysozyme at an equivalent *absolute* charge (+8 vs -10). At the initial stage of adsorption, a two-slice structure is already evident. The first slice d_1 reaches saturation after around 4 to 6 h, while slices d_2 and d_3 continue to build and reorganize over longer times. After 10h, the total thickness of the adsorbed layer has grown to about 90 Å. The R/R_F curve shows an oscillation that appears more distinct (see SI-4). Nevertheless, even though the total adsorption density appears to approach a near-equilibrium plateau, the internal structure may still be evolving.

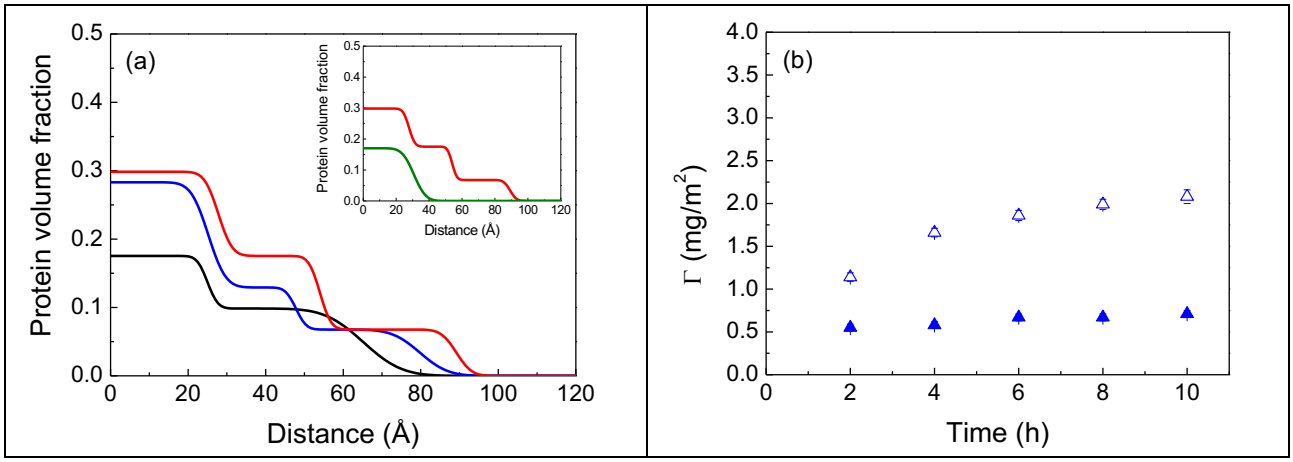

Figure 6. Adsorption of ovalbumin measured by neutron reflectivity (without advective flow) at pD 7 (net charge -10). (a) Concentration profiles at *I* = 20 mM after 2h (black line), 4h (blue line), 10h (red line); the inset compares concentration profiles after 10h for *I* = 20 mM (red line) and 170 mM (green line). (b) Adsorption density versus time at *I* = 20 mM (open circles) and *I* = 170 mM (closed circles).

The evolution of Γ with time (shown on Fig.6) barely reaches a constant value after 10 h of adsorption, similarly to lysozyme. The maximum value of $\Gamma \approx 2.1$ mg·m^{-2} is compatible with a monolayer [43,44]. The total adsorption is higher compared to the one at pD 3.6 at 20 mM (<1 mg·m^{-2})

Corresponding author sylvie.beaufils@univ-rennes1.fr

which could result from a lower *absolute* charge at pD 7.0 (- 10 e at pH 7 versus + 28 e at pH 3.6) and thus less repulsions between the proteins as they form the interfacial layer.

Fig. 7 shows the plot of the ellipsometric angle Δ as a function of adsorption time, for ovalbumin at pH 7.0, I=20 mM, in the free surface trough (with advective flow). In these conditions, no multilayers are formed: on the contrary, the ellipsometry angle is constant after a few hours, suggesting the saturation of a monolayer. However, as for ovalbumin and lysozyme in the other conditions but in the similar free surface trough, we find again a very rapid initial adsorption with an ellipsometric angle $\Delta > 5°$ at short times.

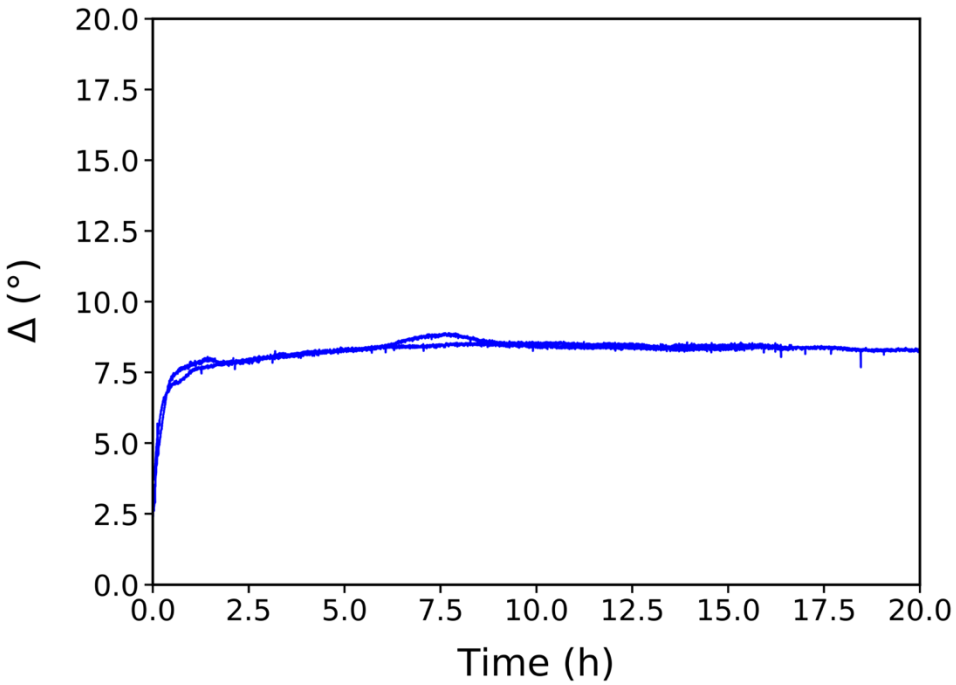

Figure 7 Ellipsometric measurements in free surface trough (*i.e.* with advection flow): ellipsometric angle Δ of ovalbumin at pH 7.0, I = 20 mM. Two replicates are drawn together.

Negatively charged ovalbumin, adsorption at high ionic strength

Surprisingly, when the ionic strength is increased, without advective flow, the adsorption is decreased significantly; in this case, due to the low signal, a one-slice model is sufficient to fit the neutron reflectivity profile. The adsorbed layer is decreased both in thickness and in density, the saturation value of the excess surface concentration being close to 0.7 mg·m^{-2} (Fig. 6, R/R_F curves given in SI-

Corresponding author sylvie.beaufils@univ-rennes1.fr

4 and SI-5). This result is contrary to the expected effect of charge screening, which decreases electrostatic repulsion between neighbouring molecules. Several elements can be taken into account to explain this effect (image charge, absolute value of the protein charge, charge of the interface, nature of buffer ions) and would require a more in depth study to go further.

Advection combined with positively charged protein are both necessary to produce multilayers

The objective of this paper was to examine the effect of a permanent interfacial advection flow on the thickness and structure of a protein air-water interfacial film that forms versus time, with a specific focus on the relation between the film properties and the charge properties of the protein involved. The most important result of our study is the evidence that the *combined effect* of the two factors, namely the *permanent advection* flow and a *positive* net electrical charge of the protein, induces the formation of a multilayer interfacial film. If one of these two factors is missing, multilayers do not form and only the 'trivial' formation of a protein monolayer is observed.

We obtain this result through experiments performed using neutron reflectivity and ellipsometry. In the conditions given above, i.e., with positively charged lysozyme (+ 8 e at pH 7.0) or ovalbumin (+ 28 e at pH 3.6), and in the presence of a permanent advective flow towards the surface, both experimental techniques indicate that film grows in a non-saturating way over several hours, well above the classical thickness of a monolayer.

The thickness of the film, estimated by neutron measurements is as high as 14 nm in the case of lysozyme (see SI-1). If we suppress the advection flow, positively charged lysozyme and ovalbumin cease to form multilayers but form monolayers, as shown on Fig. 2 and Fig. 5, respectively. If this time we conserve the advection flow but switch the sign of ovalbumin from positive to negative (- 10 e at pH 7), the protein also ceases to form multilayers and simply adsorb as a 'classical' interfacial monolayer.

Corresponding author sylvie.beaufils@univ-rennes1.fr

The classical advection-diffusion model does not predict multilayers formation

In a first attempt to explain our results, it seems important - if not mandatory - to examine if a classical advection-diffusion model is capable of describing the adsorption kinetics of the multilayer films, *once the first interfacial layer is formed*. The advection-diffusion equation is the combination of diffusion and convection (advection) equations that describes in this case the particle transport inside the physical system formed by the bulk solution and the air-water interface.

To adjust experimental kinetics of surface concentration vs time, the following points must be considered : i) as the model only describes the evaporation-driven protein advection towards the interface and does not account for the adsorption-driven irreversible formation of the first interfacial monolayer, the monolayer is then considered as the interface ii) since the experimental measurements are only sensitive to the surface concentration *excess*, we fit the difference $[C(x=0,t) - C_{bulk}]$ to the experimental data; iii) the concentration obtained from this model (in $mg.m^{-3}$) must be integrated over a thickness h to obtain a surface concentration (in $mg.m^{-2}$).

We choose to test the advection-diffusion model for lysozyme, for which we have the most complete data set. Given the intrinsic variability of the kinetics, due to the sample itself in multilayer conditions, our objective is not to describe precisely the adsorption kinetics, but to test if the model can account for the shape of the kinetics with reasonable values for the layer thickness h and the diffusion coefficient D.

The ellipsometry angle Δ is converted in excess surface concentration using the values obtained for a monolayer: $\Delta = 10°$ [45] corresponding to $\Gamma = 2\ mg/m^2$ [46]. The order of magnitude of the thickness can be estimated from neutron reflectivity measurements in presence of an advective flow (Fig. 2): $h_{exp\text{-}neutron} = 14$ nm after several hours while the diffusion coefficient of lysozyme in water is around $D_{free} = 10^{-10}\ m^2.s^{-1}$ [46].

Corresponding author sylvie.beaufils@univ-rennes1.fr

Fig. 8 shows the experimental ellipsometric angle Δ together with the value predicted by the model with the parameters ($h_{exp\text{-}neutron}$, D_{free}) as stated above. Clearly, in this case, the model does not predict multilayer formation. Additional couples of the parameters (D,h) are therefore tested: either we put h =14 nm and let D_{adjust} as adjustable parameter or alternatively we choose $D_{free} = 10^{-10}$ $m^2.s^{-1}$ and we let h_{adjust} as adjustable parameters. The results show that none of these conditions are satisfactory: if h is equal to the thickness estimated by neutron reflectivity, the adjusted diffusion coefficient is very low and, more problematically, the model does not describe the curvature of the experimental kinetics. On the contrary, if D is fixed to the free diffusion coefficient $D_{free} = 10^{-10}$ $m^2.s^{-1}$, the curvature of the experimental kinetics is correctly described, but the thickness used to estimate the surface concentration excess ($7.1\ 10^{-6}$ m) has to be more than two orders of magnitude higher that the experimental one. This trend indicates that the model, with constant diffusion coefficient, cannot describe at the same time spatial and temporal gradients. Additional examples are shown in Supp. Mat. Fig. SI-6.

Corresponding author sylvie.beaufils@univ-rennes1.fr

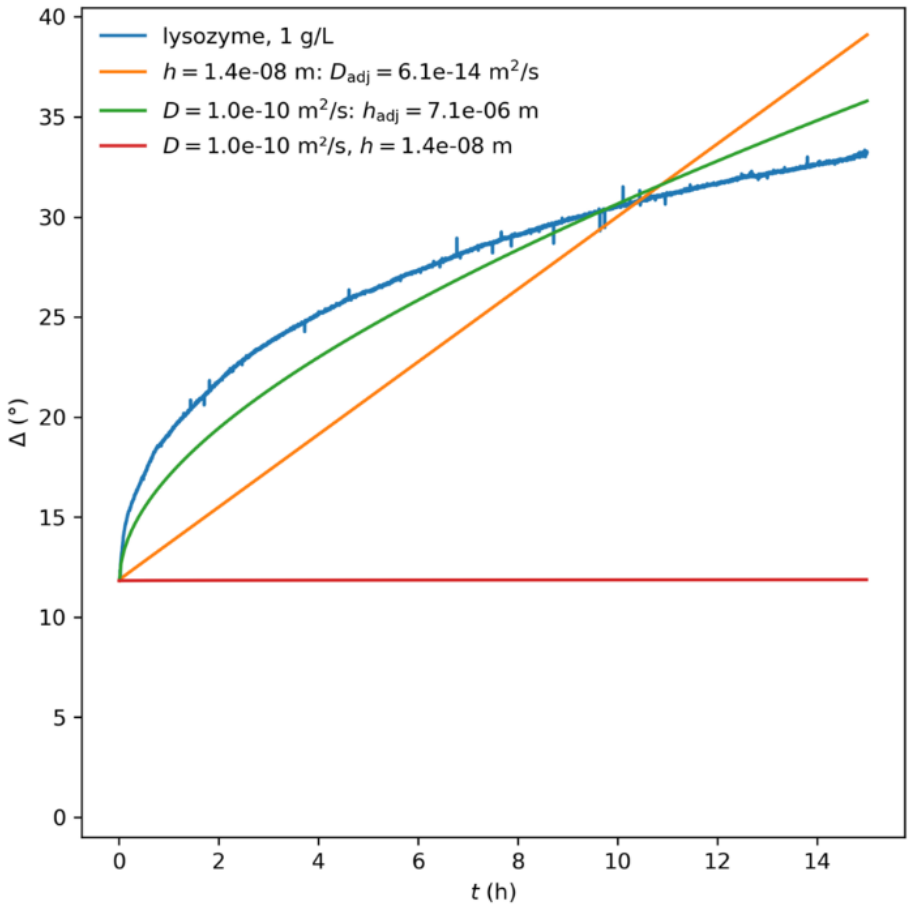

Figure 8 Fit of the advection/diffusion model to the experimental adsorption kinetics of lysozyme measured by ellipsometry, pH 7.0 (20 mM), blue curve, (a) D fixed to the free diffusion coefficient $D_{free} = 10^{-10}\ m^2.s^{-1}$, thickness fixed to the value measured by neutron reflectivity $h_{neutron}$ = 14 nm (red curve) (b) D adjusted by the model , thickness fixed to the value measured by neutron reflectivity $h_{neutron}$ = 14 nm (orange curve), (c) D fixed to the free diffusion coefficient $D_{free} = 10^{-10}\ m^2.s^{-1}$, thickness h adjusted by the model (green curve)

We conclude that the advection/diffusion model, that is based on the basic competition between advection towards the interface (due to the evaporation flow) and diffusion towards the bulk cannot describe correctly the experimental kinetics. In other words, the model tells us that, in the absence of any other effect, diffusion should be able to counterbalance by orders of magnitude the transport toward the interface due to evaporation, thus and preventing the formation of multilayers.

A possible limitation of our model is the hypothesis of a concentration-independent diffusion coefficient, whereas it is known that collective dynamics may arise between colloids at high concentration

Corresponding author sylvie.beaufils@univ-rennes1.fr

due to direct interactions between the objects[47,48], thus resulting in a change in the diffusion coefficient. We therefore, we test a model with a diffusion coefficient D(Φ) that depends on concentration in the volume fraction range $[0.1 - 0.5]$. D(Φ) is calculated from osmotic stress measurements performed in a previous study[49] on lysozyme solutions, following the formalism detailed in Bacchin (2002)[48] for colloidal particles. The equation is numerically solved using Mathematica toolbox. Using the thickness $h_{exp\text{-}neutron}$ = 14 nm, the graph C(t) versus time is flat, similar to the red curve on figure 8 (data not shown). In other words, the advection-diffusion model, even with a concentration-dependent coefficient D(Φ) estimated from osmotic stress data, cannot describes either the formation of a protein multilayer.

In our case, the mean volume fraction estimated by neutron reflectivity in the sublayer region is around Φ = 0.15 and corresponds, in the experimental pressure-volume fraction diagram, to the concentration regime where the very first signs of attractive interactions are observed in bulk. However, in this latter work, it does not produce aggregation nor bulk instability, while aggregation seems to occur near the interfacial layer upon evaporation in the present case, leading to multilayers. Such a distinction between bulk instability and surface-induced instability could be reminiscent of the observations of Linse and Wennerström[50], who have shown that attractive interactions could result in multilayer adsorption even if they are not strong enough to induce bulk aggregation.

We propose that the net charge of ovalbumin and of lysozyme, which should *a priori* induce electrostatic repulsion and is thus unfavourable to a local increase of protein concentration, yet allows attractive protein-protein interactions when it is positively charged (+ 28 e for ovalbumin and +8 e for lysozyme), as revealed at the interface upon advection and in accordance with the osmotic pressure measurements we already reported[49].

If however ovalbumin is negatively charged, the presence of an advection flow does not induce multilayers but, on the contrary monolayers (Fig. 7) as shown by the typical value of the ellipsometric angle, typical of monolayer values (close to 10°). Such an asymmetry cannot be tested for lysozyme

Corresponding author sylvie.beaufils@univ-rennes1.fr

which is positively charged at all experimental pH (its pI being about 10.7). However, this trend has been evidenced on ovotransferrin which forms multilayers when positively charged[51] and monolayer when negatively charged[52].

All these results and observation together suggest that protein-protein interaction is repulsive (or at least not attractive) for negatively charged ovalbumin and prevents the formation of multilayers after the formation of the first interfacial layer, despite the advection flow which brings proteins towards the interface.

Note that multilayer adsorption involving proteins has been thoroughly described, e.g. in the case of cooperative adsorption of multiple components, under conditions of mutual attractive interactions[53]. It forms the basis of layer-by-layer biopolymer deposition onto solid surfaces[54]. Mixed biopolymers are commonly used to stabilize food dispersed systems[55]. We also have described cooperative adsorption in a binary system of globular proteins[56,57].

Far from these conditions, for *single-protein* systems, multilayer adsorption at the air-water interface has essentially been observed under conditions of minimal repulsions at the isoelectric point *p*H[34] or at high ionic strength[58] in the presence of protein aggregates in the bulk solution[59] or in the presence of denaturant[60].

Far from the isoelectric point pH, multilayers formed by single-protein solutions were only mentioned for positively charged lysozyme at pH 7.0[2,19], for positively charged ovotransferin[51] and for negatively charged beta and kappa casein[21] while the propensity of ovalbumin to form multilayers when carrying a net positive charge, shown in this report, has never been mentioned before to our knowledge.

Hence, for globular proteins, when the specific conditions mentionned above are not met, monolayer adsorption at the air-water interface is commonly encountered[61–63].

The fact that the main result of the present work - advection flow leads to the formation of multilayers protein films at the air-water interface for positive proteins only - is essentially new in the field can

Corresponding author sylvie.beaufils@univ-rennes1.fr

possibly be explained by a few reasons. First, the adsorbed amount of proteins must be monitored on a surface exposed to the ambient atmosphere for at least several hours for being able to detect multilayers formation, which is not usual. Second, a positive net charge is not frequently found in the domain of protein adsorption kinetic measurements at the air-buffer interface. Apart from the basic lysozyme, most of the studied proteins studied in food science are acidic proteins (ovalbumin, ovotransferrin, beta-casein, beta-lactoglobulin, to cite a few) and are consequently negatively charged at a pH close to neutrality. These proteins would be positively charged at acidic pH (around 4.0). However, first, adsorption measurements are scarce in these conditions and the conditions mentioned above (free surface and several hours of kinetics) are never simultaneously fulfilled.

The asymmetric interfacial behaviour of positively and negatively charged proteins raises interesting questions, which would need a specific experimental approach, that is clearly beyond the scope of the present work. However, we may hypothesize that a part of the answer lies in the asymmetric strength of interaction of hydrated cations and anions with the side-chains of amino-acids and backbone of polypeptides[64]. This ion-specific effect is described by Okur for instance[65]: ions are ordered by their ability to salt out proteins (the Hofmeister series [66–68]) due to local interaction of ions with their surface, cations and anions being inversely ordered. Hence, the attractive interaction between proteins, leading to multilayers, would be non-symmetrically modulated by the ions present in the buffer. Following this idea and taking into account the phenomenon of charge regulation[69,70] would certainly allow to go further.

CONCLUSION

The presence of an advection flow, together with a positive electric charge of the protein, are necessary conditions to observe multilayers formation with lysozyme or ovalbumin solutions. The presence of multilayers may be explained by the presence of attractive protein-protein interactions in these conditions, as it is also found in the bulk through the equation of state of lysozyme established

Corresponding author sylvie.beaufils@univ-rennes1.fr

by Pasquier in comparable ionic conditions[49]. So the positive charge of ovalbumin and of lysozyme, which is a priori unfavourable to an increase in local concentration, yet seems to induce attractive protein-protein interactions in particular situations. An important difference between the bulk and the interface is that those attractive interactions lead to bulk lysozyme crystallization in the first case, while we have no evidence of crystallization of lysozyme during multilayers formation at the interface, although we cannot definitively rule it out.

For negatively charged ovalbumin, the formation of multilayers after the formation of the first interfacial layer is not observed, even in the presence of an advection flow and we have the classical monolayer formation reported in the literature. So in this case, and even with advection, protein-protein interactions stay repulsive in these conditions - which is the a-priori situation.

These results suggest that interfacial multilayers induced by advection flow strongly depends on the sign of the protein charge. This hypothesis should now be checked with a wider range of proteins in various conditions of charge, both in terms of sign and absolute value.

Supporting Information

Neutron reflectivity measurements, Normalized reflectivity.

Figure SI-1 showing the Kinetics of adsorption of lysozyme from D_2O at pD 7 (net charge +8) and *I*=20 mM measured by neutron reflectivity in open trough (with advective flow).

Figure SI-2 showing the Effect of NaCl on adsorption of lysozyme measured by neutron reflectivity in airtight trough (without advective flow) at pD 7 (net charge +8) after 10h.

Figure SI-3 showing the Effect of NaCl on adsorption of ovalbumin measured by neutron reflectivity (without advective flow) at pD 3.6 (net charge +28) after 10h.

Figure SI-4 showing the Kinetics of adsorption of ovalbumin measured by neutron reflectivity (without advective flow) at pD 7 (net charge +28) and *I* = 20 mM.

Figure SI-5 showing Effect of NaCl on adsorption of ovalbumin measured by neutron reflectivity (without advective flow) at pD 7 (net charge -10) after 10h.

Corresponding author sylvie.beaufils@univ-rennes1.fr

Resolution of the advection-diffusion model

Details on resolution the advection-diffusion model.

Figure SI-6 showing the Fit of the advection/diffusion model to the experimental adsorption kinetics of lysozyme measured by ellipsometry, pH 7.0 (20 mM)

Figure SI-7 showing a photograph of the trough used for neutron reflectivity measurements

Table T-1 showing the estimated charges of ovalbumin

Corresponding author sylvie.beaufils@univ-rennes1.fr

	Time (h)	Slab n	$d \pm 2$ (Å)	$\phi_p \pm 0.02$	Γ (mg.m^{-2})
Lysozyme					
pD = 7, I = 20 mM (airtight trough, no advection)	2	1	24	0.29	1.27 ± 0.04
		2	22	0.08	
	4	1	25	0.36	1.63 ± 0.04
		2	38	0.06	
	6	1	23	0.38	1.79 ± 0.05
		2	38	0.10	
	8	1	22	0.42	1.99 ± 0.05
		2	28	0.12	
		3	22	0.06	
	10	1	24	0.36	2.02 ± 0.06
		2	25	0.16	
		3	37	0.05	
	12	1	23	0.42	2.09 ± 0.04
		2	17	0.16	
		3	27	0.08	
	14	1	23	0.40	2.02 ± 0.05
		2	23	0.12	
		3	26	0.08	
	16	1	24	0.38	1.97 ± 0.05
		2	32	0.12	
		3	15	0.06	
pD = 7, I = 170 mM (airtight trough, no advection)	2	1	20	0.38	1.65 ± 0.04
		2	42 ± 3	0.09	
	4	1	25	0.36	2.02 ± 0.05
		2	33	0.15	
	6	1	27	0.42	2.40 ± 0.05
		2	18	0.17	
		3	43 ± 3	0.06	
	8	1	25	0.42	2.40 ± 0.04
		2	24	0.17	
		3	24	0.09	
	10	1	25	0.40	2.39 ± 0.04
		2	25	0.19	
		3	24	0.09	
pD = 7, I = 20 mM (without cover, advection)	1	1	23	0.35 ± 0.02	1.57 ± 0.09
		2	61 ± 5	0.04 ± 0.02	
	2	1	27	0.39 ± 0.03	2.21 ± 0.11
		2	49 ± 5	0.10 ± 0.03	
	3	1	29	0.33 ± 0.03	2.57 ± 0.26
		2	21	0.18 ± 0.03	
		3	78 ± 9	0.06 ± 0.03	
	4	1	23	0.40 ± 0.03	2.76 ± 0.25
		2	27	0.23 ± 0.03	

Corresponding author sylvie.beaufils@univ-rennes1.fr

		3	69 ± 6	0.06 ± 0.03	
	5	1	28	0.37 ± 0.03	2.83 ± 0.27
		2	21	0.22 ± 0.03	
		3	65 ± 5	0.07 ± 0.03	
	6	1	22	0.36 ± 0.04	2.98 ± 0.28
		2	24	0.32 ± 0.04	
		3	57 ± 5	0.09 ± 0.04	
	7	1	30	0.39 ± 0.05	3.20 ± 0.32
		2	19	0.28 ± 0.05	
		3	41 ± 4	0.13 ± 0.05	
Ovalbumin					
pD = 7, I = 20 mM (airtight trough, no advection)	2	1	25	0.18	1.14 ± 0.05
		2	40	0.10	
	4	1	25	0.28	1.66 ± 0.05
		2	23	0.13	
		3	32	0.07	
	6	1	23	0.30	1.86 ± 0.06
		2	23	0.14	
		3	30	0.11	
	8	1	25	0.30	1.99 ± 0.06
		2	30	0.16	
		3	28	0.08	
	10	1	28	0.30	2.08 ± 0.08
		2	26	0.18	
		3	35	0.07	
pD = 7, I = 170 mM (airtight trough, no advection)	2	1	29	0.14	0.55 ± 0.04
	4	1	28	0.15	0.58 ± 0.04
	6	1	32	0.15	0.67 ± 0.04
	8	1	32	0.15	0.67 ± 0.04
	10	1	31	0.17	0.71 ± 0.04
pD = 3.6, I = 20 mM (airtight trough, no advection)	2	1	27	0.11	0.40 ± 0.04
	4	1	25	0.11	0.37 ± 0.04
	6	1	24	0.15	0.51 ± 0.03
	8	1	21	0.14	0.41 ± 0.03
	10	1	26	0.14	0.50 ± 0.03
pD = 3.6, I = 170 mM (airtight trough, no advection)	2	1	22	0.15	0.67 ± 0.11
		2	50 ± 5	0.03	
	4	1	22	0.19	0.75 ± 0.10
		2	50 ± 5	0.03	
	6	1	21	0.20	0.86 ± 0.13
		2	66 ± 6	0.03	
	8	1	18	0.22	0.85 ± 0.13

Corresponding author sylvie.beaufils@univ-rennes1.fr

		2	72 ± 7	0.03	
	10	1	24	0.20	0.89 ± 0.12
		2	54 ± 5	0.03	

Table I Fitted values corresponding to the results of Figure 1,2,3 4 and 6.

References

(1) Graham, D. E.; Phillips, M. C. Proteins at Liquid Interfaces. *J. Colloid Interface Sci.* **1979**, *70* (3), 403–414.

(2) Graham, D. E.; Phillips, M. C. Proteins at Liquid Interfaces: II. Adsorption Isotherms. *J. Colloid Interface Sci.* **1979**, *70* (3), 415–426.

(3) Fainerman, V. B.; Lucassen-Reynders, E. H.; Miller, R. Adsorption of Surfactants and Proteins at Fluid Interfaces. *Colloids Surf. Physicochem. Eng. Asp.* **1998**, *143* (2–3), 141–165.

(4) Fainerman, V. B.; Lucassen-Reynders, E. H.; Miller, R. Description of the Adsorption Behaviour of Proteins at Water/Fluid Interfaces in the Framework of a Two-Dimensional Solution Model. *Adv. Colloid Interface Sci.* **2003**, *106* (1–3), 237–259.

(5) Dickinson, E. Milk Protein Interfacial Layers and the Relationship to Emulsion Stability and Rheology. *Colloids Surf. B Biointerfaces* **2001**, *20* (3), 197–210.

(6) Dickinson, E. Hydrocolloids at Interfaces and the Influence on the Properties of Dispersed Systems. *Food Hydrocoll.* **2003**, *17* (1), 25–39.

(7) Dickinson, E. Hydrocolloids Acting as Emulsifying Agents–How Do They Do It? *Food Hydrocoll.* **2018**, *78*, 2–14.

(8) Berton-Carabin, C. C.; Sagis, L.; Schroën, K. Formation, Structure, and Functionality of Interfacial Layers in Food Emulsions. *Annu. Rev. Food Sci. Technol.* **2018**, *9*, 551–587.

(9) Berton-Carabin, C.; Schroën, K. Towards New Food Emulsions: Designing the Interface and Beyond. *Curr. Opin. Food Sci.* **2019**, *27*, 74–81.

(10) Wierenga, P. A.; Gruppen, H. New Views on Foams from Protein Solutions. *Curr. Opin. Colloid Interface Sci.* **2010**, *15* (5), 365–373.

(11) Narsimhan, G.; Xiang, N. Role of Proteins on Formation, Drainage, and Stability of Liquid Food Foams. *Annu. Rev. Food Sci. Technol.* **2018**, *9*, 45–63.

(12) Andrade, J. D.; Hlady, V.; Wei, A. P.; Ho, C. H.; Lea, A. S.; Jeon, S. I.; Lin, Y. S.; Stroup, E. Proteins at Interfaces: Principles, Multivariate Aspects, Protein Resistant Surfaces, and Direct Imaging and Manipulation of Adsorbed Proteins. In *Biologically modified polymeric biomaterial surfaces*; Springer, 1992; pp 67–84.

(13) Schor, M.; Reid, J. L.; MacPhee, C. E.; Stanley-Wall, N. R. The Diverse Structures and Functions of Surfactant Proteins. *Trends Biochem. Sci.* **2016**, *41* (7), 610–620.

(14) Saxena, A.; Tripathi, B. P.; Kumar, M.; Shahi, V. K. Membrane-Based Techniques for the Separation and Purification of Proteins: An Overview. *Adv. Colloid Interface Sci.* **2009**, *145* (1–2), 1–22.

(15) Brans, G.; Schroën, C.; Van der Sman, R. G. M.; Boom, R. M. Membrane Fractionation of Milk: State of the Art and Challenges. *J. Membr. Sci.* **2004**, *243* (1–2), 263–272.

(16) Aguero, R.; Bringas, E.; San Román, M. F.; Ortiz, I.; Ibanez, R. Membrane Processes for Whey Proteins Separation and Purification. A Review. *Curr. Org. Chem.* **2017**, *21* (17), 1740–1752.

(17) Soodam, K.; Guinee, T. P. The Case for Milk Protein Standardisation Using Membrane Filtration for Improving Cheese Consistency and Quality. *Int. J. Dairy Technol.* **2018**, *71* (2), 277–

Corresponding author sylvie.beaufils@univ-rennes1.fr

291.
(18) Beier, S. P.; Enevoldsen, A. D.; Kontogeorgis, G. M.; Hansen, E. B.; Jonsson, G. Adsorption of Amylase Enzyme on Ultrafiltration Membranes. *Langmuir* **2007**, *23* (18), 9341–9351.
(19) Yano, Y. F. Kinetics of Protein Unfolding at Interfaces. *J. Phys. Condens. Matter* **2012**, *24* (50), 503101.
(20) Sutherland, K. L. The Kinetics of Adsorption at Liquid Surfaces. *Aust. J. Chem.* **1952**, *5* (4), 683–696.
(21) Benjamins, J.; De Feijter, J. A.; Evans, M. T. A.; Graham, D. E.; Phillips, M. C. Dynamic and Static Properties of Proteins Adsorbed at the Air/Water Interface. *Faraday Discuss. Chem. Soc.* **1975**, *59*, 218–229.
(22) Davies, R. J.; Goodwin, G. C.; Lyle, I. G.; Jones, M. N. The Behaviour of Glycophorin at the Air—Water Interface. *Colloids Surf.* **1983**, *8* (1), 29–43.
(23) Fournier, J. B.; Cazabat, A. M. Tears of Wine. *EPL Europhys. Lett.* **1992**, *20* (6), 517.
(24) Deegan, R. D.; Bakajin, O.; Dupont, T. F.; Huber, G.; Nagel, S. R.; Witten, T. A. Capillary Flow as the Cause of Ring Stains from Dried Liquid Drops. *Nature* **1997**, *389* (6653), 827–829.
(25) Dhavaleswarapu, H. K.; Migliaccio, C. P.; Garimella, S. V.; Murthy, J. Y. Experimental Investigation of Evaporation from Low-Contact-Angle Sessile Droplets. *Langmuir* **2010**, *26* (2), 880–888.
(26) Kim, G.; Gurau, M.; Kim, J.; Cremer, P. S. Investigations of Lysozyme Adsorption at the Air/Water and Quartz/Water Interfaces by Vibrational Sum Frequency Spectroscopy. *Langmuir* **2002**, *18* (7), 2807–2811.
(27) Roberts, S. A.; Kellaway, I. W.; Taylor, K. M.; Warburton, B.; Peters, K. Combined Surface Pressure− Interfacial Shear Rheology Study of the Effect of PH on the Adsorption of Proteins at the Air− Water Interface. *Langmuir* **2005**, *21* (16), 7342–7348.
(28) Wierenga, P. A.; Meinders, M. B.; Egmond, M. R.; Voragen, A. G.; de Jongh, H. H. Quantitative Description of the Relation between Protein Net Charge and Protein Adsorption to Air− Water Interfaces. *J. Phys. Chem. B* **2005**, *109* (35), 16946–16952.
(29) Hartvig, R. A. Vd W., M.; Østergaard, J.; Jorgensen, L.; Jensen, H. *Langmuir* **2011**, *27* (6), 2634–2643.
(30) Liao, Z.; Lampe, J. W.; Ayyaswamy, P. S.; Eckmann, D. M.; Dmochowski, I. J. Protein Assembly at the Air–Water Interface Studied by Fluorescence Microscopy. *Langmuir* **2011**, *27* (21), 12775–12781.
(31) Boström, M.; Tavares, F. W.; Finet, S.; Skouri-Panet, F.; Tardieu, A.; Ninham, B. W. Why Forces between Proteins Follow Different Hofmeister Series for PH above and below PI. *Biophys. Chem.* **2005**, *117* (3), 217–224.
(32) Hartvig, R. A. Vd W., M.; Østergaard, J.; Jorgensen, L.; Jensen, H. *Langmuir* **2011**, *27* (6), 2634–2643.
(33) Hartvig, R. A.; van de Weert, M.; Østergaard, J.; Jorgensen, L.; Jensen, H. Formation of Dielectric Layers and Charge Regulation in Protein Adsorption at Biomimetic Interfaces. *Langmuir* **2012**, *28* (3), 1804–1815.
(34) Engelhardt, K.; Rumpel, A.; Walter, J.; Dombrowski, J.; Kulozik, U.; Braunschweig, B.; Peukert, W. Protein Adsorption at the Electrified Air–Water Interface: Implications on Foam Stability. *Langmuir* **2012**, *28* (20), 7780–7787.
(35) Croguennec, T.; Nau, F.; Pezennec, S.; Brule, G. Simple Rapid Procedure for Preparation of Large Quantities of Ovalbumin. *J. Agric. Food Chem.* **2000**, *48* (10), 4883–4889.
(36) Dolinsky, T. J.; Nielsen, J. E.; McCammon, J. A.; Baker, N. A. PDB2PQR: An Automated Pipeline for the Setup of Poisson-Boltzmann Electrostatics Calculations. *Nucleic Acids Res.* **2004**, *32* (Web Server), W665–W667. https://doi.org/10.1093/nar/gkh381.
(37) Olsson, M. H. M.; Søndergaard, C. R.; Rostkowski, M.; Jensen, J. H. PROPKA3: Consistent Treatment of Internal and Surface Residues in Empirical PKa Predictions. *J. Chem. Theory Comput.*

Corresponding author sylvie.beaufils@univ-rennes1.fr

2011, *7* (2), 525–537. https://doi.org/10.1021/ct100578z.
(38) Covington, A. K.; Paabo, M.; Robinson, R. A.; Bates, R. G. Use of the Glass Electrode in Deuterium Oxide and the Relation between the Standardized PD (PaD) Scale and the Operational PH in Heavy Water. *Anal. Chem.* **1968**, *40* (4), 700–706.
(39) Born, M.; Wolf, E. *Principles of Optics (Pergamon Press, Oxford)(Ruse. Transls*; Nauka, M, 1970.
(40) Crowley, T. L. A Uniform Kinematic Approximation for Specular Reflectivity. *Phys. Stat. Mech. Its Appl.* **1993**, *195* (3–4), 354–374.
(41) Lu, J. R.; Lee, E. M.; Thomas, R. K. The Analysis and Interpretation of Neutron and X-Ray Specular Reflection. *Acta Crystallogr. A* **1996**, *52* (1), 11–41.
(42) Van Alstine, J. M.; Malmsten, M.; Brooks, D. E. Poly (Ethylene Glycol) Amphiphile Adsorption and Liposome Partition. *J. Chromatogr. B. Biomed. Sci. App.* **1996**, *680* (1–2), 145–155.
(43) De Feijter, J. A.; Benjamins, J.; Veer, F. A. Ellipsometry as a Tool to Study the Adsorption Behavior of Synthetic and Biopolymers at the Air–Water Interface. *Biopolym. Orig. Res. Biomol.* **1978**, *17* (7), 1759–1772.
(44) De Feijter, J. A.; Benjamins, J. Adsorption Kinetics of Proteins at the Air-Water Interface. *Food Emuls. Foams* **1987**, 72–85.
(45) Pezennec, S.; Gauthier, F.; Alonso, C.; Graner, F.; Croguennec, T.; Brule, G.; Renault, A. The Protein Net Electric Charge Determines the Surface Rheological Properties of Ovalbumin Adsorbed at the Air–Water Interface. *Food Hydrocoll.* **2000**, *14* (5), 463–472.
(46) Xu, S.; Damodaran, S. The Role of Chemical Potential in the Adsorption of Lysozyme at the Air-Water Interface. *Langmuir* **1992**, *8* (8), 2021–2027.
(47) Bowen, W. R.; Liang, Y.; Williams, P. M. Gradient Diffusion Coefficients—Theory and Experiment. *Chem. Eng. Sci.* **2000**, *55* (13), 2359–2377.
(48) Bacchin, P.; Si-Hassen, D.; Starov, V.; Clifton, M. J.; Aimar, P. A Unifying Model for Concentration Polarization, Gel-Layer Formation and Particle Deposition in Cross-Flow Membrane Filtration of Colloidal Suspensions. *Chem. Eng. Sci.* **2002**, *57* (1), 77–91.
(49) Pasquier, C.; Beaufils, S.; Bouchoux, A.; Rigault, S.; Cabane, B.; Lund, M.; Lechevalier, V.; Le Floch-Fouéré, C.; Pasco, M.; Pabœuf, G. Osmotic Pressures of Lysozyme Solutions from Gas-like to Crystal States. *Phys. Chem. Chem. Phys.* **2016**, *18* (41), 28458–28465.
(50) Linse, P.; Wennerström, H. Adsorption versus Aggregation. Particles and Surface of the Same Material. *Soft Matter* **2012**, *8* (8), 2486–2493.
(51) Le Floch-Fouéré, C.; Pezennec, S.; Pasco, M.; Paboeuf, G.; Renault, A.; Beaufils, S. Moderate Conformational Impact of Citrate on Ovotransferrin Considerably Increases Its Capacity to Self-Assemble at the Interface. *J. Colloid Interface Sci.* **2015**, *437*, 219–226.
(52) Le Floch-Fouéré, C.; Pezennec, S.; Pézolet, M.; Rioux-Dubé, J.-F.; Renault, A.; Beaufils, S. Unexpected Differences in the Behavior of Ovotransferrin at the Air–Water Interface at PH 6.5 and 8.0. *J. Colloid Interface Sci.* **2011**, *356* (2), 614–623.
(53) Holmberg, M.; Hou, X. Competitive Protein Adsorption Multilayer Adsorption and Surface Induced Protein Aggregation. *Langmuir* **2009**, *25* (4), 2081–2089.
(54) vander Straeten, A.; Lefèvre, D.; Demoustier-Champagne, S.; Dupont-Gillain, C. Protein-Based Polyelectrolyte Multilayers. *Adv. Colloid Interface Sci.* **2020**, *280*, 102161. https://doi.org/10.1016/j.cis.2020.102161.
(55) Dickinson, E. Mixed Biopolymers at Interfaces: Competitive Adsorption and Multilayer Structures. *Food Hydrocoll.* **2011**, *25* (8), 1966–1983.
(56) Le Floch-Fouéré, C.; Pezennec, S.; Lechevalier, V.; Beaufils, S.; Desbat, B.; Pézolet, M.; Renault, A. Synergy between Ovalbumin and Lysozyme Leads to Non-Additive Interfacial and Foaming Properties of Mixtures. *Food Hydrocoll.* **2009**, *23* (2), 352–365. https://doi.org/10.1016/j.foodhyd.2008.01.007.

Corresponding author sylvie.beaufils@univ-rennes1.fr

(57) Le Floch-Fouéré, C.; Beaufils, S.; Lechevalier, V.; Nau, F.; Pézolet, M.; Renault, A.; Pezennec, S. Sequential Adsorption of Egg-White Proteins at the Air–Water Interface Suggests a Stratified Organization of the Interfacial Film. *Food Hydrocoll.* **2010**, *24* (4), 275–284. https://doi.org/10.1016/j.foodhyd.2009.10.006.
(58) Georganopoulou, D. G.; Williams, D. E.; Pereira, C. M.; Silva, F.; Su, T.-J.; Lu, J. R. Adsorption of Glucose Oxidase at Organic− Aqueous and Air− Aqueous Interfaces. *Langmuir* **2003**, *19* (12), 4977–4984.
(59) Rullier, B.; Axelos, M. A. V.; Langevin, D.; Novales, B. β-Lactoglobulin Aggregates in Foam Films: Correlation between Foam Films and Foaming Properties. *J. Colloid Interface Sci.* **2009**, *336* (2), 750–755. https://doi.org/10.1016/j.jcis.2009.04.034.
(60) Perriman, A. W.; Henderson, M. J.; Evenhuis, C. R.; McGillivray, D. J.; White, J. W. Effect of the Air−Water Interface on the Structure of Lysozyme in the Presence of Guanidinium Chloride. *J. Phys. Chem. B* **2008**, *112* (31), 9532–9539. https://doi.org/10.1021/jp800354r.
(61) Theodoratou, A.; Lee, L.-T.; Oberdisse, J.; Aubert-Pouëssel, A. Equilibrium Protein Adsorption on Nanometric Vegetable Oil Hybrid Film/Water Interface Using Neutron Reflectometry. *Langmuir* **2019**, *35* (20), 6620–6629. https://doi.org/10.1021/acs.langmuir.9b00186.
(62) Hähl, H.; Griffo, A.; Safaridehkohneh, N.; Heppe, J.; Backes, S.; Lienemann, M.; Linder, M. B.; Santen, L.; Laaksonen, P.; Jacobs, K. Dynamic Assembly of Class II Hydrophobins from T. Reesei at the Air–Water Interface. *Langmuir* **2019**, *35* (28), 9202–9212. https://doi.org/10.1021/acs.langmuir.9b01078.
(63) Delahaije, R. J. B. M.; Gruppen, H.; Giuseppin, M. L. F.; Wierenga, P. A. Quantitative Description of the Parameters Affecting the Adsorption Behaviour of Globular Proteins. *Colloids Surf. B Biointerfaces* **2014**, *123*, 199–206. https://doi.org/10.1016/j.colsurfb.2014.09.015.
(64) Lund, M.; Vácha, R.; Jungwirth, P. Specific Ion Binding to Macromolecules: Effects of Hydrophobicity and Ion Pairing. *Langmuir* **2008**, *24* (7), 3387–3391.
(65) Okur, H. I.; Hladílková, J.; Rembert, K. B.; Cho, Y.; Heyda, J.; Dzubiella, J.; Cremer, P. S.; Jungwirth, P. Beyond the Hofmeister Series: Ion-Specific Effects on Proteins and Their Biological Functions. *J. Phys. Chem. B* **2017**, *121* (9), 1997–2014. https://doi.org/10.1021/acs.jpcb.6b10797.
(66) Jungwirth, P.; Tobias, D. J. Specific Ion Effects at the Air/Water Interface. *Chem. Rev.* **2006**, *106* (4), 1259–1281.
(67) Jungwirth, P.; Winter, B. Ions at Aqueous Interfaces: From Water Surface to Hydrated Proteins. *Annu Rev Phys Chem* **2008**, *59*, 343–366.
(68) Jungwirth, P.; Cremer, P. S. Beyond Hofmeister. *Nat. Chem.* **2014**, *6* (4), 261–263.
(69) Lund, M.; Jönsson, B. On the Charge Regulation of Proteins. *Biochemistry* **2005**, *44* (15), 5722–5727.
(70) Lund, M.; Jönsson, B. Charge Regulation in Biomolecular Solution. *Q. Rev. Biophys.* **2013**, *46* (3), 265–281.

Corresponding author sylvie.beaufils@univ-rennes1.fr

Graphic for Table of Contents

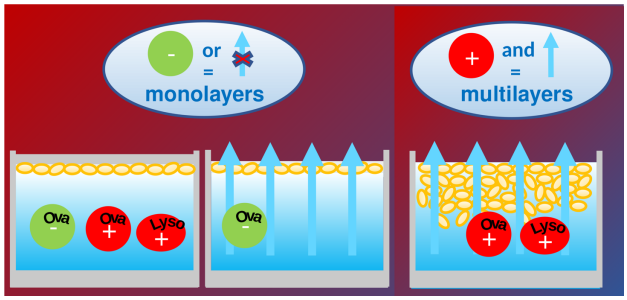

Corresponding author sylvie.beaufils@univ-rennes1.fr